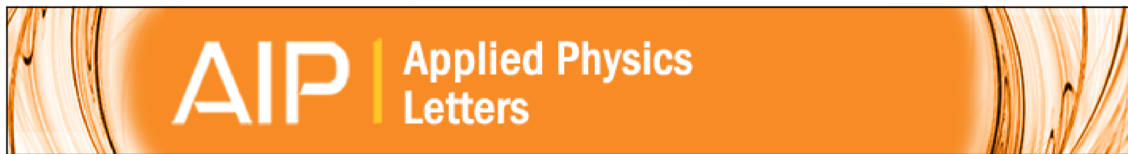

Low-temperature ion-induced epitaxial growth of α-FeSi2 and cubic FeSi2 in Si

X. W. Lin, M. Behar, J. Desimoni, H. Bernas, J. Washburn, and Z. Liliental-Weber

Citation: Applied Physics Letters **63**, 105 (1993); doi: 10.1063/1.109727
View online: http://dx.doi.org/10.1063/1.109727
View Table of Contents: http://scitation.aip.org/content/aip/journal/apl/63/1?ver=pdfcov
Published by the AIP Publishing

Articles you may be interested in

Composition dependence of activation energy in solid phase epitaxial growth of Si1−x Ge x alloys
J. Appl. Phys. **80**, 6716 (1996); 10.1063/1.363745

Kinetics of solid phase epitaxy in buried amorphous Si layers formed by MeV ion implantation
Appl. Phys. Lett. **69**, 925 (1996); 10.1063/1.116945

Sequential phase formation by ion-induced epitaxy in Fe-implanted Si(001). Study of their properties and thermal behavior
J. Appl. Phys. **79**, 752 (1996); 10.1063/1.360821

Epitaxial growth of (001) Al on (111) Si by vapor deposition
Appl. Phys. Lett. **61**, 913 (1992); 10.1063/1.107726

Epitaxial growth of rare-earth silicides on (111) Si
Appl. Phys. Lett. **48**, 466 (1986); 10.1063/1.96532

NEW Special Topic Sections
NOW ONLINE
Lithium Niobate Properties and Applications: Reviews of Emerging Trends
AIP Applied Physics Reviews

Reuse of AIP Publishing content is subject to the terms at: https://publishing.aip.org/authors/rights-and-permissions. Download to IP: 143.54.44.137 On: Thu, 05 May 2016 17:42:07

Low-temperature ion-induced epitaxial growth of α-$FeSi_2$ and cubic $FeSi_2$ in Si

X. W. Lin
Materials Science Division, Lawrence Berkeley Laboratory, University of California at Berkeley, Berkeley, California 94720

M. Behar,[a] J. Desimoni,[b] and H. Bernas
Centre de Spectromètrie Nucléaire et Spectromètrie de Masse, Bât. 108, 91405 Orsay Campus, France

J. Washburn and Z. Liliental-Weber
Materials Science Division, Lawrence Berkeley Laboratory, University of California at Berkeley, Berkeley, California 94720

(Received 22 December 1992; accepted for publication 25 March 1993)

Ion-beam-induced epitaxial crystallization of amorphous Si implanted with Fe to 18 at. % peak concentration was studied. The structure of the specimen was characterized using transmission electron microscopy and Rutherford backscattering spectrometry. Both cubic $FeSi_2$ and α-$FeSi_2$ were formed in epitaxy with the Si matrix with two types of orientations (fully aligned and twinned). The twins of α-$FeSi_2$ and those of cubic $FeSi_2$ were found to have exactly the same type of epitaxial relationship as for the aligned ones. The thermodynamically stable β-$FeSi_2$ is not formed, demonstrating that ion-beam-induced crystallization can lead to preferential phase formation as well as to epitaxy.

To date, much effort has been devoted to the study of the epitaxy of β-$FeSi_2$ on Si because it is a semiconductor that exhibits a direct transition at a band gap of ≈ 0.9 eV and thus of great interest for optoelectronic devices.[1–3] Only limited work, however, has been reported for the other two $FeSi_2$ phases which are very different from β-$FeSi_2$ in many aspects. α-$FeSi_2$ is a metallic tetragonal phase stable above ≈ 950 °C, as opposed to β-$FeSi_2$ which is orthorhombic and stable at temperatures below ≈ 950 °C.[3,4] The newly discovered cubic $FeSi_2$ phase[2,5–10] is metallic and, probably, magnetic[5,10] with a fluorite structure ($a_c \approx a_{Si} = 0.5431$ nm) that can be produced only under restricted conditions. Crystallographic analysis indicates that the α phase is better lattice matched with Si than the β phase, while the cubic phase is best matched with Si among the three $FeSi_2$ phases, because of $a_c \approx a_{Si}$. In the case of α-$FeSi_2$ ($a_\alpha = b_\alpha = 0.2695$ nm and $c_\alpha = 0.514$ nm), since $2a_\alpha = 0.5390$ nm, the lattice mismatch between α-$FeSi_2$ and Si or cubic $FeSi_2$ is only 0.7% along the a or b axis, as compared to a mismatch of $\approx 2\%$ for β-$FeSi_2$ grown epitaxially on a Si substrate.[11]

The first reported cubic $FeSi_2$ phase was obtained either by molecular beam epitaxy (MBE) combined with solid phase epitaxy[5] or by reactive deposition epitaxy[6] on a Si(111) substrate. This phase is metastable and transforms into β-$FeSi_2$ upon annealing. The transition temperature was found to decrease with increasing thickness of the epilayer.[5] For a 30-nm-thick layer, the transition temperature is ≈ 200 °C. This result indicates that the interface energy between the epilayer and the substrate plays a crucial role in stabilizing the cubic $FeSi_2$ phase. More recently, we have reported the formation of cubic $FeSi_2$ in an Fe-implanted Si by an ion-beam-induced epitaxial crystallization (IBIEC) process.[9] In that case, the gain in interface energy is larger, because the cubic $FeSi_2$ is formed as small particles (diameter ≈ 5 nm) buried in the Si matrix and thus has a greater interface-to-volume ratio than a thin film grown on Si. The cubic phase precipitates were found to be stable above 520 °C. Moreover, two types of precipitates were observed, i.e., A-type and B-type precipitates, corresponding to full alignment of cubic $FeSi_2$ with the Si matrix and twinning along {111} of A type, respectively. In this letter, we present a study of Si implanted with Fe to a high dose (≈ 18 at. %), using transmission electron microscopy (TEM) and Rutherford backscattering spectrometry combined with channeling (RBS/C). It demonstrates, for the first time, not only the epitaxial formation of the high-temperature α-$FeSi_2$ phase by IBIEC at a low temperature (320 °C), but also the coexistence of this phase with cubic $FeSi_2$ in Si.

Si(001) wafers (p type, 1 Ω cm) were implanted with 50-keV Fe^+ ions to a fluence of 4×10^{16} cm^{-2} (≈ 18 at. % at the peak concentration). During implantation, the specimens were maintained at room temperature and channeled implantation was avoided. The Fe-implanted amorphous layer was crystallized by IBIEC, i.e., by irradiating the specimens at 320 °C with 500-keV Si^+ ions to a fluence of 7.2×10^{16} cm^{-2}; the beam flux was 1 μA cm^{-2}.

The structure was characterized using cross-sectional TEM, including selected-area diffraction (SAD). TEM specimens were prepared by mechanical polishing and ion milling. The same specimens were also studied by RBS/C with a 1.2-MeV $^4He^+$ beam aligned randomly and the channeling direction (Si [001]), using a standard goniometer arrangement.

The RBS/C spectra (not shown) from Si indicate that

[a]On leave from Instituto de Fisica, UFRGS, Porto Alegre, Brazil.
[b]On leave from Departmento de Fisica, Facultad de Ciencias Exactas, UNLP, under a fellowship from CONICET, Argentina.

Reuse of AIP Publishing content is subject to the terms at: https://publishing.aip.org/authors/rights-and-permissions. Download to IP: 143.54.44.137 On: Thu, 05 May 2016 17:42:07

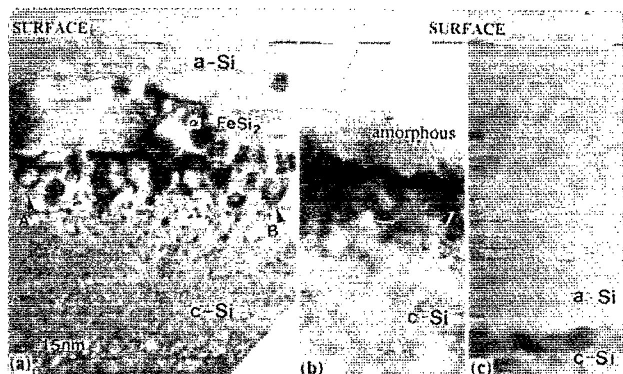

FIG. 1. Cross-sectional TEM micrographs of Si implanted at room temperature with 18 at. % Fe peak concentration, showing the phase distribution after different treatments at 320 °C: (a) After Si^+ irradiation to 7.2×10^{16} cm^{-2}. Under the α-$FeSi_2$ layer are aligned (A-type) and twin-oriented (B-type) cubic $FeSi_2$ precipitates, as indicated by arrows A and B. (b) After Si^+ irradiation to 3.6×10^{16} cm^{-2}. Below the amorphous top layer are cubic $FeSi_2$ precipitates, as indicated by arrows. (The weak contrast of the precipitates is because they are in a relatively thick area.) (c) After thermal annealing only. The thick layer above c-Si is completely amorphous.

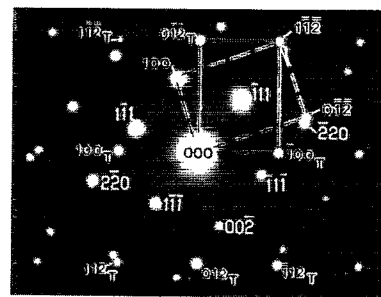

FIG. 2. A SAD pattern taken from a lower interface area of the α-$FeSi_2$ layer shown in Fig. 1(a). The diffraction spots correspond to the reflections from the [110] zone axis of Si or A-type cubic $FeSi_2$ (white indices) and from the $[0\bar{2}1]$ zone axis of two α-$FeSi_2$ crystals (outlined black indices) twinned along $(1\bar{1}\bar{2})$. The spots indicated by the dashed and the solid lines correspond to an α-$FeSi_2$ grain in epitaxy with Si and its twin (indices with subscript T), respectively.

the initial Fe implantation produces an amorphous Si (a-Si) layer $\approx$100-nm thick and that the subsequent ion irradiation promotes crystallization and reduces this a-Si layer by $\approx$40 nm. On the other hand, the Fe peak indicates the formation of an Fe-containing region $\approx$35-nm wide and a Gaussian-like distribution of Fe atoms. The IBIEC process causes only a slight narrowing of the Fe peak; neither peak shift nor channeling effect is observed.

TEM observation of the same ion-irradiated specimen reveals a layered structure. The TEM image in Fig. 1(a) shows that the specimen consists of a surface amorphous Si layer (a-Si) $\approx$15 nm thick[12] above an α-$FeSi_2$ layer ($\approx$20 nm thick) and a crystalline Si (c-Si) region which contains spherical-shaped cubic $FeSi_2$ precipitates over a width of $\approx$40 nm. These cubic $FeSi_2$ particles decrease in size and, at the same time, increase in number density with increasing depth. The typical diameter of the cubic $FeSi_2$ particles is $\approx$10 nm adjacent to the interface with α-$FeSi_2$, but rapidly decreases to $\approx$1 nm at a greater depth. The A-type and B-type cubic $FeSi_2$ precipitates, previously found in a Si implanted to a low Fe dose ($\approx$5 at. %),[9] are also observed [indicated by the arrows in Fig. 1(a)]. Note that, while the large particles adjacent to the lower interface of α-$FeSi_2$ are of both A type and B type, the small particles in the lower region are predominantly of A type.

The phase distribution in the specimen is related to the Fe concentration profile. Comparison between the TEM and the RBS/C data shows that the α-$FeSi_2$ layer is located around the Fe profile peak, whereas the cubic $FeSi_2$ phase region corresponds to the tail of the Fe profile. This relationship leads to three observations.

First, since cubic $FeSi_2$ precipitates are only found at the profile tail, their formation must be associated with a low Fe concentration, in agreement with our previous results.[9]

Second, the size and density of cubic $FeSi_2$ precipitates vary as a function of Fe concentration, i.e., the decrease of Fe concentration at the profile tail results in a decrease in size and an increase in density of the precipitates. Moreover, their orientation tends to change from A type to B type, as the Fe concentration (hence the precipitate size) increases. This implies that for the small particles (<3 nm in diameter), A-type orientation is more stable than B type.

Third, the formation of the α-$FeSi_2$ layer around the peak of the Fe profile suggests that there exists a size limit for the growth of cubic $FeSi_2$ beyond which the cubic phase becomes unstable and a new phase grows in lieu of cubic $FeSi_2$. The existence of such a stability limit was already apparent for cubic $FeSi_2$ epilayers grown on Si(111) surface by MBE and the stable phase of the epilayers was β-$FeSi_2$, in agreement with the equilibrium phase diagram.[5] The major difference here is the absence of the β phase and the formation of the α phase at a temperature $\approx$600 °C below its equilibrium stability limit.

The α-$FeSi_2$ layer consists of grains with a diameter ranging from 20 to 100 nm. Some are in epitaxy with the underlying Si or A-type cubic $FeSi_2$ and others are twinned with respect to the epitaxial one along the α-$FeSi_2$\{112\} planes. Figure 2(a) shows a typical SAD pattern taken from an area including α-$FeSi_2$, Si, and cubic $FeSi_2$. From this pattern the orientation relationship between the epitaxial α-$FeSi_2$ grains and Si (or A-type cubic $FeSi_2$) is determined as α-$FeSi_2$ $[0\bar{2}1]\|$Si[110] and α-$FeSi_2$ (100)$\|$Si(002). This relationship implies that the b and c axes of the α-$FeSi_2$ unit cell are lying in a plane parallel to Si (001), i.e., the lower interface of the α-$FeSi_2$ layer, and are virtually parallel to the b and a axes of Si (or A-type cubic $FeSi_2$), respectively, because the angle between the b_α and b_{Si} axes (or c_α and a_{Si}) is only 1.3°. Thus, the lattice mismatch in the interface is $\approx$0.7% and 5% along α-$FeSi_2$ [010] and [001], respectively. A slight deviation from the above epitaxial relationship, i.e., a relative rotation of two parallel planes by an angle (θ) up to $\approx$3°, is often observed, such as occurs for α-$FeSi_2$ $(0\bar{1}\bar{2})$ with Si$(\bar{2}20)$ ($\theta \approx 3°$) in Fig. 2. This rotation explains the absence of channeling for the Fe peak in the RBS/C spectra.

Reuse of AIP Publishing content is subject to the terms at: https://publishing.aip.org/authors/rights-and-permissions. Download to IP: 143.54.44.137 On: Thu, 05 May 2016 17:42:07

In Fig. 2, one also finds the diffraction spots from the α-$FeSi_2$ grains twinned along $(1\bar{1}\bar{2})$. We find that all the twin-oriented grains of α-$FeSi_2$ layer have the same type of orientation relationship as shown above with respect to twin-oriented cubic $FeSi_2$ particles (B type). In fact, since $2a_\alpha \approx a_c$ and $c_\alpha \approx a_c$, the twin planes {112} of α-$FeSi_2$ are equivalent to the twin planes {111} of cubic $FeSi_2$. This indicates that the twinned α-$FeSi_2$ phase is formed in epitaxy with the B-type cubic $FeSi_2$, same as the epitaxial α-$FeSi_2$ phase with the A-type cubic $FeSi_2$.

In order to check that the α and cubic phases are selectively formed in the IBIEC process, we performed two complementary experiments, in which two samples were prepared under conditions identical to those described above, except as regards the following. In one case, IBIEC with 3.6×10^{16} Si^+ cm^{-2} was performed in order to recrystallize roughly half the as-implanted amorphous layer. No $FeSi_2$ precipitate is found in the remaining amorphous layer ($\approx$35 nm thick) [Fig. 1(b)], proving that $FeSi_2$ precipitates are formed only when the Si is recrystallized. In the other case, no IBIEC was performed, but the sample was annealed at 320 °C for 3.2 h, i.e., a duration identical to that of the IBIEC procedure with 7.2×10^{16} Si^+ cm^{-2}. No thermally induced cyrstallization occurs at all (amorphous layer $\approx$95 nm) [Fig. 1(c)], indicating that IBIEC is indispensable for $FeSi_2$ precipitation at 320 °C. These two experiments also prove that no precipitation occurs at all during Fe implantation at room temperature.

From the thermodynamic point of view, the formation of α-$FeSi_2$ at 320 °C by IBIEC is surprising, because this phase is stable only at high temperatures ($>\approx$950 °C), as opposed to the low-temperature β-$FeSi_2$ phase which is stable below $\approx$950 °C. The mechanism of the α-$FeSi_2$ phase formation warrants discussion. IBIEC is a nonequilibrium process for which kinetic factors may be important. This process involves epitaxial growth of a crystal with the crystalline-amorphous (*c-a*) interface migrating toward the surface at a speed depending on irradiation flux and temperature.[13] In our case, the crystallization speed of Si is measured as $\approx$1.5 nm min^{-1}. Obviously, in this crystallization process, epitaxial growth of Si is favored, because it involves a lower interfacial energy than growth in a random orientation. For the same reason, when $FeSi_2$ is involved in the crystallization process, not only its orientation, but also its phase, may be determined by the underlying crystal structure, especially when the precipitate dimension is small and the interfacial energy makes a significant contribution to the total free energy of the system.

As the *c-a* interface moves toward the surface, the cubic $FeSi_2$ phase is first formed at the tail of the Fe profile, because it is small in size and the interfacial energy is minimized by matching with the Si matrix, as in the case of a thin epilayer grown on a Si substrate.[5–7] As the *c-a* interface approaches the peak of the Fe profile, the size of the cubic precipitates increases rather rapidly to such a point that the decrease in interfacial energy by lattice matching with Si is insufficient to maintain the stability of the cubic phase and, consequently, a phase with a lower volume free energy, and possibly also a lower strain energy begins to grow. If we assume that the interfacial energy is also the controlling factor for nucleation of this new phase, α-$FeSi_2$, rather than β-$FeSi_2$, should be formed, because it has a better lattice match with Si or cubic $FeSi_2$ than β-$FeSi_2$. The strongest evidence in support of this epitaxial growth mechanism is the fact that all the grains in the α-$FeSi_2$ layer are found to be in perfect alignment with either the A-type or the B-type cubic $FeSi_2$ with exactly the same orientation relationship.

We are grateful for the technical assistance provided by the Semiramis Group (Orsay). The electron microscopy studies reported in this work were supported by the Director, Office of Energy Research, U.S. Department of Energy under Contract No. DE-AC0376 SF00098. We wish to thank W. Swider for her help in TEM specimen preparation, and C. Clerc, F. Fortuna, M. O. Ruault, J. Chevrier, and J. Derrien for valuable comments.

[1] H. C. Cheng, T. R. Yew, and L. J. Chen, J. Appl. Phys. **57**, 5246 (1985); M. C. Bost and J. E. Mahan, *ibid.* **64**, 2034 (1988); D. J. Oostra, D. E. W. Vandenhoudt, C. W. T. Bulle-Lieuwma, and E. P. Naburgh, Appl. Phys. Lett. **59**, 1737 (1991); J. Derrien, J. Chevrier, V. Le Thanh, and J. E. Mahan, Appl. Surf. Sci. **56–58**, 382 (1992); C. Giannini, S. Lagomarsino, F. Scarinci, and P. Castrucci, Phys. Rev. B **45**, 8822 (1992); S. Mantl, Mater. Sci. Rep. **8**, 1 (1992), and references therein.
[2] J. Alvarez, J. J. Hinarejos, E. G. Michel, G. R. Castro, and R. Miranda, Phys. Rev. B **45**, 14042 (1992).
[3] K. Radermacher, S. Mantl, Ch. Dieker, and H. Lüth, Appl. Phys. Lett. **59**, 2145 (1991).
[4] U. Birkholz and J. Schelm, Phys. Status Solidi **34**, K177 (1969); Y. Dusausoy, J. Protas, R. Wandji, and B. Roques, Acta Cryst. B **27**, 1209 (1971).
[5] N. Onda, J. Henz, E. Müller, K. A. Mäder, and H. von Känel, Appl. Surf. Sci. **56–58**, 421 (1992); H. von Känel, K. A. Mäder, E. Müller, N. Onda, and H. Sirringhaus, Phys. Rev. B **45**, 13807 (1992).
[6] V. Le Thanh, J. Chevrier, and J. Derrien, Phys. Rev. B **46**, 15946 (1992).
[7] H. Moritz, B. Rösen, S. Popovic, A. Rizzi, and H. Lüth, J. Vac. Sci. Technol. B **10**, 1704 (1992).
[8] M. G. Grimaldi, P. Baeri, C. Spinella, and S. Lagomarsino, Appl. Phys. Lett. **60**, 1132 (1992).
[9] J. Desimoni, H. Bernas, M. Behar, X. W. Lin, J. Washburn, and Z. Liliental-Weber, Appl. Phys. Lett **62**, 306 (1993); J. Desimoni, M. Behar, H. Bernas, X. W. Lin, Z. Liliental-Weber, and J. Washburn, Nucl. Instrum. Methods (to be published).
[10] N. E. Christensen, Phys. Rev. B **42**, 7148 (1990).
[11] N. Cherief, C. D'Anterroches, R. C. Cinti, T. A. Nguyen Tan, and J. Derrien, Appl. Phys. Lett. **55**, 1671 (1989); J. Mahan, K. M. Geib, G. Y. Robinson, R. G. Long, X. Yan, G. Bai, and M.-A. Nicolet, *ibid.* **56**, 2126 (1990).
[12] Using our experimental pure Si recrystallization speed ($\approx$1.5 nm min^{-1}), complete recrystallization would be expected for the IBIEC fluence used here. The observed *a*-Si layer is presumably due to blocking of the crystallization front by the α-$FeSi_2$ layer.
[13] J. Linnros, B. Svensson, and G. Holmén, Phys. Rev. B **30**, 3629 (1984).

Reuse of AIP Publishing content is subject to the terms at: https://publishing.aip.org/authors/rights-and-permissions. Download to IP: 143.54.44.137 On: Thu, 05 May 2016 17:42:07